ELECTRON TRANSFER AND EXCITATION IN COLLISIONS BETWEEN HEAVY ELEMENT IMPURITY IONS AND HELIUM ATOMS

V. K. Nikulin, N. A. Guschina

Devision of Plasma Physics, Atomic Physics and Astrophysics
A.F.Ioffe Physical-Technical Institute,
St.Petersburg, 194021, Russia

Research Co-ordination Meeting
on C R P
" Atomic data for heavy element impurities
in fusion reactors"

26–28 September 2007, IAEA, Vienna, Austria

OUTLINE:

Summary

Recent results of our theoretical studies of charge transfer in collisions involving heavy element ions, helium atoms, and alpha-particles are reviewed.

New theoretical data on the partial and total cross sections for electron transfer, transfer excitation and excitation for collisions of Ti^{4+}, Cr^{6+}, and Fe^{8+} ions with helium atoms in the ground states were obtained [1–3] by using the close-coupling method with thirteen (Ti^{4+}) and eleven (Cr^{6+}, Fe^{8+}) two-electron quasimolecular states in the energy range of impurity ions from 4 to 400 keV.

The partial and total cross sections of electron transfer into n-shells of the Ti^{3+} (n=5–8), Cr^{6+} (n=6–9), and Fe^{8+} (n=8–11) ions were calculated [4, 5] for collisions of the impurity ions with helium atoms in metastable states with basis of seventeen (Ti^{4+}) and ten (Cr^{6+}, Fe^{8+}) one-electron quasimolecular states.

The cross sections of alpha particle neutralization through quasi-resonant double electron capture in slow collisions with C^{2+} and Ti^{2+} ions were calculated. New data on the partial and total cross sections for electron transfer and target excitation in collisions of alpha particles with the Be-like oxygen ions were obtained [6] in the energy range of 0.2 to 2 MeV.

The above calculations were performed by solving the close-coupling equations on the basis of thirteen (O^{4+}) and nine (C^{2+}) four-electron and of thirteen (Ti^{2+}) two-electron quasimolecular states.

Data on the cross sections are needed both for simulating the behaviour of alpha particles in plasma and for the plasma core spectroscopic diagnostics. The emission from the excited metallic impurities and helium ions produced in the collisions are of interest for the plasma edge diagnostics.

Pioneer theoretical data for the single-electron charge transfer and excitations due to collisions between Bi^{4+} ions in the ground (6s)and metastable (6p) states were obtained [7, 8] in the collision energy interval 5–75 keV in the center-of-mass frame. Gaining insight into charge transfer between identical low-charged heavy ions at their collisions due to betatron oscillations is vital to designing accelerators and storage rings with the aim to generate intense ion beams [9]. Such beams can also find application in heavy-ion-driven inertial fusion.

The calculations were carried out by using our computer program package [10] for the treatment inelastic processes in slow ion-atom collisions in the framework of the close-coupling equation method involving basis of many-electron quasimolecular states.

2. Theoretical method

The study of charge transfer and excitation reactions was performed by the use of the close-coupling equation method with two- or many-electron quasi-molecular states ϕ_i as a basis. Coulomb trajectories were used to integrate coupled equations using code TANGO provided us by A. Salin [11].

Two-electron wave function ϕ_i for the orthonormal one-electron basis ψ_k may be represented in the form

$$\phi_i(\vec{r}_k,\vec{r}_l) \;=\; \frac{1}{\sqrt{2}}[\psi_k(\vec{r}_k)\psi_l(\vec{r}_l) \pm \psi_k(\vec{r}_l)\psi_l(\vec{r}_k)] \;\; (\pm - \textbf{singlet, triplet cases}) \;, \quad (2.1)$$

where ψ_k may be obtained within the effective potential method. Our effective potential [12] takes into account a screening of nucleus by electrons

$$V_{eff}(R,\vec{r}_j) = \frac{1}{2}\left[\frac{a_1-b_1}{r_{1j}} + \frac{a_1+b_1}{r_{2j}} + \frac{\tilde{a}_1+Ra_0}{r_{1j}r_{2j}} + \frac{b_2(r_{1j}-r_{2j})^2}{Rr_{1j}r_{2j}}\right] \quad (2.2)$$

and allows for the separation of variables in the one-electron Schödinger equation in prolate spheroidal coordinate system

$$h\psi_k(\vec{r}_j) \;=\; \left[-\frac{\nabla_j^2}{2} - \frac{Z_1}{r_{1j}} - \frac{Z_2}{r_{2j}} + V_{eff}(\vec{R},r_{1j},r_{2j})\right]\psi_k(\vec{r}_j) = \varepsilon_k(R)\psi_k(\vec{r}_j) \;, \quad (2.3)$$

where R is the internuclear distance and r_{1j} and r_{2j} are the distances from the $\vec{r}_j$ electron to the nuclei with charges Z_1 and Z_2, respectively; a_0, $\tilde{a}_1$, a_1, b_1, and b_2 are the effective potential parameters.

If V_{eff}=0 we have the H_2^+ problem and the One Electron Diatomic Molecular Orbitals (OEDMO) with hidden symmetry. In our method Screened Diatomic Molecular Orbitals (SDMO), ψ_k has the same symmetry.

The SDMO basis was used for calculating the total energies E_i, for example of the two-electron or many-electron diabatic states

$$E_i \;=\; <\phi_i|H|\phi_i> = \varepsilon_k + \varepsilon_l + J^c_{kl} \pm J^{ex}_{kl} - (V^k_{eff} + V^l_{eff}) \;, \quad (2.4)$$

$$H \;=\; \sum_{j=k,l}\left[-\frac{\nabla_j^2}{2} - \frac{Z_1}{r_{1j}} - \frac{Z_2}{r_{2j}}\right] + \frac{1}{r_{kl}} \;. \quad (2.5)$$

Here J^c_{kl}, and J^{ex}_{kl} are Coulomb and exchanged integrals; V^k_{eff} and V^l_{eff} are diagonal matrix elements of the effective potential.

The many-electron energies are calculated in fact to the first one order of the perturbation theory in the residual interaction W=$1/r_{kl}$ − $V_{eff}(\vec{r}_k)$ − $V_{eff}(\vec{r}_l)$.

The matrix elements of dynamic and potential couplings are obtained using the calculated basis SDMO. To take into account electron momentum transfer, the matrix elements are calculated for origin placed at centre of charges of colliding ions.

3. Close-coupling calculation of electron transfer and transfer excitation cross sections in collisions of Ti^{4+}, Cr^{6+}, and Fe^{8+} with helium atoms in the ground state.

The main aim of the research was to provide new theoretical data on the electron transfer and excitation processes in collisions of the multiply charged metallic impurity ions of elements Ti, Cr and Fe important to present CRP with helium atoms in the ground as well as in the initially excited states. The single- and double-electron capture , transfer excitation, and excitation of helium were calculated at relative keV-collision energies important for modeling and diagnostics of the plasma edge.

Calculations of the total and partial cross sections for Ti^{4+}– He collisions in the energy range 0.1–6 MeV were performed by Fritsch [13] within the framework of the close-coupling method with regard to two active electrons also, but the important two-electron transfer excitation and DEC channels being omitted from his calculations.

We performed [1–3] the close coupling calculation of the single electron capture (SEC), transfer excitation (TE) and double electron capture (DEC), and excitation (EXC) cross sections for slow collisions:

$$\mathrm{Ti}^{4+}(3p^6) + \mathrm{He}(1s^2) \rightarrow \begin{cases} \mathrm{Ti}^{3+}(3p^6 nl) + \mathrm{He}^{+}(1s) & \text{(SEC)} \\ \qquad (n = 3, 4) & \\ \mathrm{Ti}^{3+}(3p^6 3d) + \mathrm{He}^{+}(2p) & \text{(TE)} \\ \mathrm{Ti}^{2+}(3p^6 3d^2) + \mathrm{He}^{2+} & \text{(DEC)} \\ \mathrm{Ti}^{4+}(3p^6) + \mathrm{He}(1s2l), & \text{(EXC)} \end{cases} \quad (1)$$

$$\mathrm{Cr}^{6+}(3p^6) + \mathrm{He}(1s^2) \rightarrow \begin{cases} \mathrm{Cr}^{5+}(3p^6 nl) + \mathrm{He}^{+}(1s) & \text{(SEC)} \\ \qquad (n = 4, 5) & \\ \mathrm{Cr}^{4+}(3p^6 3d5l) + \mathrm{He}^{2+} & \text{(DEC)} \\ & \\ \mathrm{Cr}^{5+}(3p^6 3d) + \mathrm{He}^{+}(2l), & \text{(TE)} \end{cases} \quad (2)$$

$$\mathrm{Fe}^{8+}(3p^6) + \mathrm{He}(1s^2) \rightarrow \begin{cases} \mathrm{Fe}^{7+}(3p^6 nl) + \mathrm{He}^{+}(1s) & \text{(SEC)} \\ \qquad (n = 4 - 7) & \\ \mathrm{Fe}^{6+}(3p^6 nln'l') + \mathrm{He}^{2+} & \text{(DEC)} \\ \qquad (n = 4, n' = 4, 5) & \\ \mathrm{Fe}^{7+}(3p^6 4f) + \mathrm{He}^{+}(2l) \ ). & \text{(TE)} \end{cases} \quad (3)$$

The thirteen, eleven and eight two-electron quasimolecular states for Ti^{4+}+He, Cr^{6+}+He, and for Fe^{8+}+He collisions are presented in Tables I – III, respectively. The calculated two-electron state correlation diagrams for $(He–Ti)^{4+}$, $(He–Cr)^{6+}$, and $(He–Fe)^{8+}$ quasimolecules are shown in Fig. 1-3.

Table I. Entrance, SEC, TE, DEC and EXC channels in the reaction (1). Energies of resonance defects ΔE_p are obtained from atomic calculations.

channel	ϕ_p	**atomic limit at R$\rightarrow \infty$**	ΔE_p **(a.u.)**
entrance	ϕ_1	$\mathbf{Ti^{4+} + He(1s^2)}$	
SEC	ϕ_9	$\mathbf{Ti^{3+}(4d) + He^{+}(1s)}$	**0.13**
	ϕ_8	$\mathbf{Ti^{3+}(4f) + He^{+}(1s)}$	**0.33**
	ϕ_4	$\mathbf{Ti^{3+}(4p) + He^{+}(1s)}$	**-0.17**
	ϕ_3	$\mathbf{Ti^{3+}(4s) + He^{+}(1s)}$	**-0.38**
	ϕ_5	$\mathbf{Ti^{3+}(3d) + He^{+}(1s)}$	**-0.72**
	ϕ_2	$\mathbf{Ti^{3+}(3d) + He^{+}(1s)}$	**-0.72**
DEC	ϕ_7	$\mathbf{Ti^{2+}}(3d_0^2) \mathbf{+ He^{2+}}$	**0.34**
	ϕ_6	$\mathbf{Ti^{2+}}(3d_0 3d_{\pm 1}) \mathbf{+ He^{2+}}$	**0.34**
EXC	ϕ_{13}	$\mathbf{Ti^{4+} + He(1s2s)}$	**0.82**
	ϕ_{12}	$\mathbf{Ti^{4+} + He(1s2p)}$	**0.86**
TE	ϕ_{11}	$\mathbf{Ti^{3+}}(3d) \mathbf{+ He^{+}}(2p_{\pm 1})$	**0.97**
	ϕ_{10}	$\mathbf{Ti^{3+}}(3d) \mathbf{+ He^{+}}(2p_0)$	**0.97**

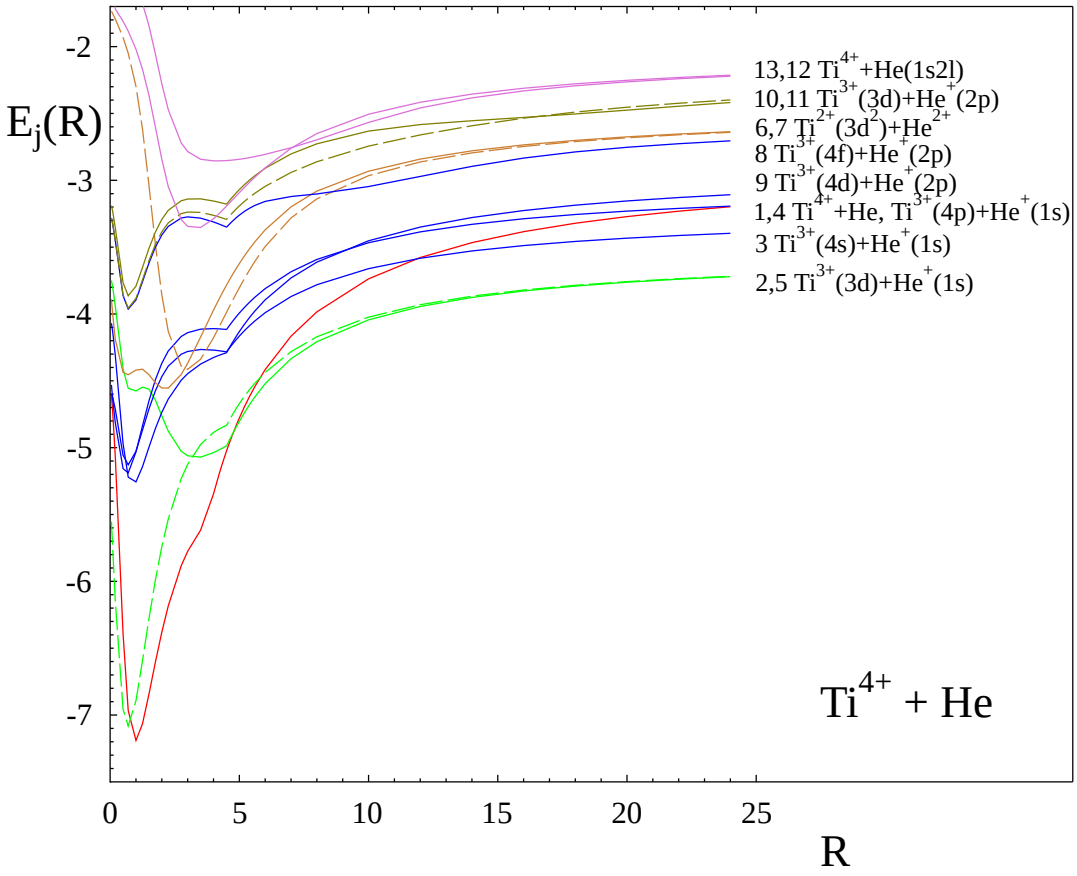

Figure 1: **The energies $\mathbf{E}_i$(R) of two-electron states $\phi_i(\psi_j, \psi_{j'})$ of the ($\mathbf{Ti^{4+}}$+He) quasimolecule:**
a) the entrance channel (red curve) – $\phi_1(3d\sigma', 3d\sigma')$;
b) the channels of the single-electron transfer into nl-states with n=3 (green curves) and n=4 (blue curves) of $\mathbf{Ti^{3+}}$ions – $\phi_2(3d\sigma, 4f\sigma)$, $\phi_5(3d\sigma, 3d\pi)$, **and** $\phi_3(3d\sigma, 4s\sigma)$, $\phi_4(3d\sigma, 4p\sigma)$, $\phi_8(3d\sigma, 6h\sigma)$, $\phi_9(3d\sigma, 4d\sigma)$;
c) the channels of the double-electron capture into 3d-states of $\mathbf{Ti^{2+}}$ ions (gold curves) – $\phi_6(4f\sigma', 4f\sigma')$, $\phi_7(4f\sigma', 3d\pi)$;
d) the transfer excitation channels (the single-electron transfer into 3d-states of $\mathbf{Ti^{3+}}$ ion with the simultaneous electron 1s→ 2p excitation of He atom) (olive curves) – $\phi_{10}(4f\sigma, 5g\sigma)$, $\phi_{11}(4f\sigma, 4f\pi)$;
d) the channels of electron 1s→2s, $\mathbf{2p_0}$ excitations of He atoms (orchid curves) – $\phi_{12}(3d\sigma, 7i\sigma)$, $\phi_{13}(3d\sigma, 6g\sigma)$.

Table II. Entrance, SEC, DEC and TE channels in the reaction (2). Energies of resonance defects ΔE_p are obtained from atomic calculations.

channel	ϕ_p	**atomic limit at R $\to \infty$**	ΔE_p **(a.u.)**
entrance	ϕ_1	$\mathbf{Cr}^{6+}(3p^6)$ + $\mathbf{He}(1s^2)$	**0.**
SEC	ϕ_2	$\mathbf{Cr}^{5+}(4s)$+ $\mathbf{He}^{+}(1s)$	**-1.445**
	ϕ_3	$\mathbf{Cr}^{5+}(4p)$+ $\mathbf{He}^{+}(1s)$	**-1.142**
	ϕ_4	$\mathbf{Cr}^{5+}(4d)$+ $\mathbf{He}^{+}(1s)$	**-0.679**
	ϕ_5	$\mathbf{Cr}^{5+}(4f_0)$+ $\mathbf{He}^{+}(1s)$	**-0.330**
	ϕ_6	$\mathbf{Cr}^{5+}(4f_{\pm1})$+ $\mathbf{He}^{+}(1s)$	**-0.330**
	ϕ_7	$\mathbf{Cr}^{5+}(5f)$+ $\mathbf{He}^{+}(1s)$	**0.087**
	ϕ_8	$\mathbf{Cr}^{5+}(5g)$+ $\mathbf{He}^{+}(1s)$	**0.127**
DEC	ϕ_9	$\mathbf{Cr}^{4+}(3d5g)$ + $\mathbf{He}^{2+}$	**-0.910**
TE	ϕ_{10}	$\mathbf{Cr}^{5+}(3d)$+ $\mathbf{He}^{+}(2p)$	**-0.958**
	ϕ_{11}	$\mathbf{Cr}^{5+}(3d)$+ $\mathbf{He}^{+}(2s)$	**-0.958**

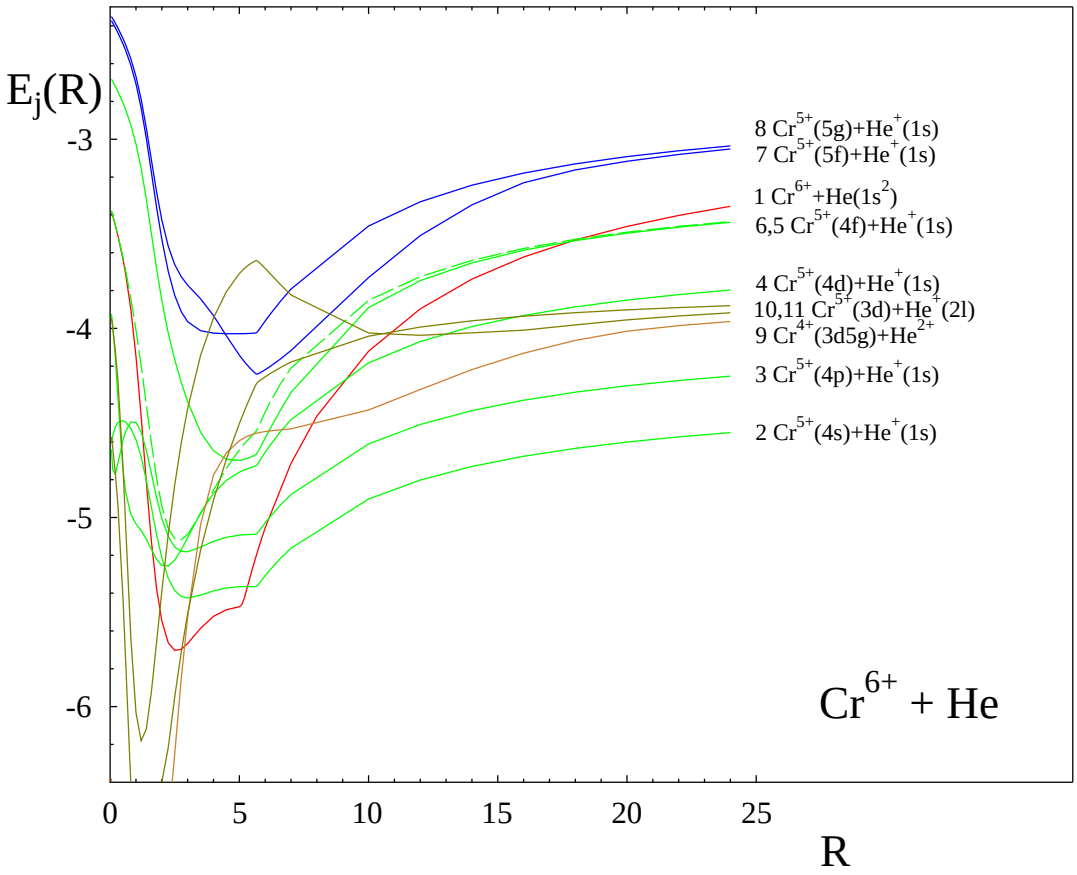

Figure 2: **The energies $\mathbf{E}_i$(R) of the two-electron states $\phi_i(\psi_j, \psi_{j'})$ of the ($\mathbf{Cr^{6+}}$+He) quasimolecule:**
a) the entrance channel(red curve) – $\phi_1(4f\sigma', 4f\sigma')$**(•);**
b) the channels of single-electron transfer into nl-states with n=4 (green curves) and n=5 (blue curves) of $\mathbf{Cr^{5+}}$ ions – $\phi_2(4s\sigma, 4f\sigma)$, $\phi_3(4p\sigma, 4f\sigma)$, **and** $\phi_4(4d\sigma, 4f\sigma)$, $\phi_5(5g\sigma, 4f\sigma)$, $\phi_6(4f\pi, 4f\sigma)$, $\phi_7(6g\sigma, 4f\sigma)$, $\phi_8(6h\sigma, 4f\sigma)$;
c) the channel of double-electron transfer into 3d5g-state of $\mathbf{Cr^{6+}}$ ions (gold curve) – $\phi_9(3d\sigma^*, 6h\sigma^*)$;
d) the transfer excitation channels (single-electron transfer into 3d-state of $\mathbf{Cr^{5+}}$ ion with the simultaneous electron 1s→ $2l$ **excitation of He atom) (olive curves) –** $\phi_{10}(3d\sigma, 7i\sigma)$, $\phi_{11}(3d\sigma, 5f\sigma)$.

Table III. Entrance, SEC, DEC and TE channels in the reaction (3). Energies of resonance defects ΔE_p are obtained from atomic calculations.

channel	ϕ_p	**atomic limit at R** $\rightarrow \infty$	ΔE_p **(a.u.)**
entrance	ϕ_1	$\mathbf{Fe}^{8+}(3p^6)$ + $\mathbf{He}(1s^2)$	**0.**
SEC	ϕ_2	$\mathbf{Fe}^{7+}(4f)$+ $\mathbf{He}^{+}(1s)$	**-1.221**
	ϕ_3	$\mathbf{Fe}^{7+}(5g)$+ $\mathbf{He}^{+}(1s)$	**-0.438**
	ϕ_4	$\mathbf{Fe}^{7+}(6h)$+ $\mathbf{He}^{+}(1s)$	**-0.003**
	ϕ_5	$\mathbf{Cr}^{7+}(7i)$+ $\mathbf{He}^{+}(1s)$	**0.417**
DEC	ϕ_6	$\mathbf{Fe}^{6+}(4f^2)$ + $\mathbf{He}^{2+}$	**-0.892**
	ϕ_7	$\mathbf{Fe}^{6+}(4f5g)$ + $\mathbf{He}^{2+}$	**-0.258**
TE	ϕ_8	$\mathbf{Fe}^{7+}(4f)$+ $\mathbf{He}^{+}(2p)$	**0.279**

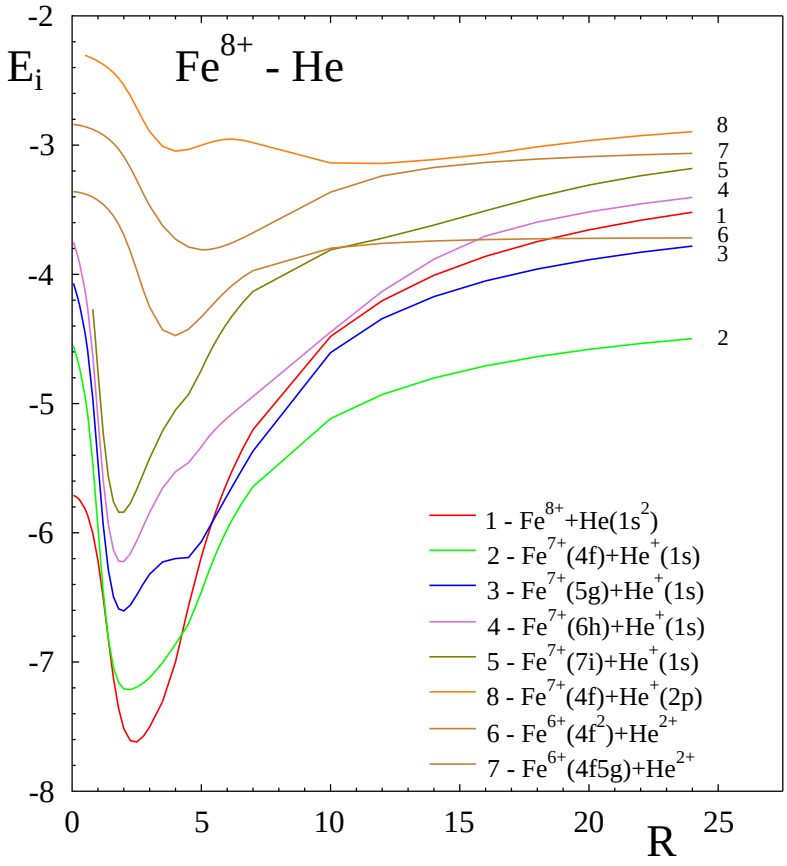

Figure 3: **The energies $\mathbf{E}_i$(R) of the two-electron states $\phi_i(\psi_j, \psi_{j'})$ of the (Fe^{8+}+He) quasimolecule:**
a) the entrance channel (red curve) – $\phi_1(4f\sigma', 4f\sigma')$**;**
b) the single-electron transfer channels into 4f- (green curve), 5g- (blue curve), 6h- (orchid curve), 7i- (olive curve) states of Fe^{7+}(nl) ions – $\phi_2(4f\sigma, 5g\sigma)$, $\phi_3(4f\sigma, 6h\sigma)$, $\phi_4(4f\sigma, 7i\sigma)$, $\phi_5(4f\sigma, 9k\sigma)$**;**
c) the double-electron transfer channels into 4f^2- and 4f5g-states of Fe^{6+} ions (gold curves) – $\phi_6(5g\sigma', 5g\sigma')$, $\phi_7(5g\sigma^*, 6h\sigma^*)$**;**
d) the channel of transfer excitation (the single-electron transfer into 4f-state of Fe^{7+} ion with the simultaneous electron 1s$\rightarrow 2p_0$ excitation of He atom) (orange curve) – $\phi_8(5g\sigma, 8j\sigma)$**.**

Results obtained

a) Ti^{4+}+ He collisions

The calculated cross sections [2] in the energy range from 2 to 400 keV are shown in Fig. 4 together with the theoretical results by Fritsch [13]. The calculation of total and partial cross sections was performed by Fritsch in the energy range 100 keV– 6 MeV within the framework of the close-coupling method using the basis set of atomic orbitals. It is clearly seen that data on the total single-electron transfer cross section obtained by us qualitatively agree with the results by Fritsch [13] in the energy range 100–150 keV.

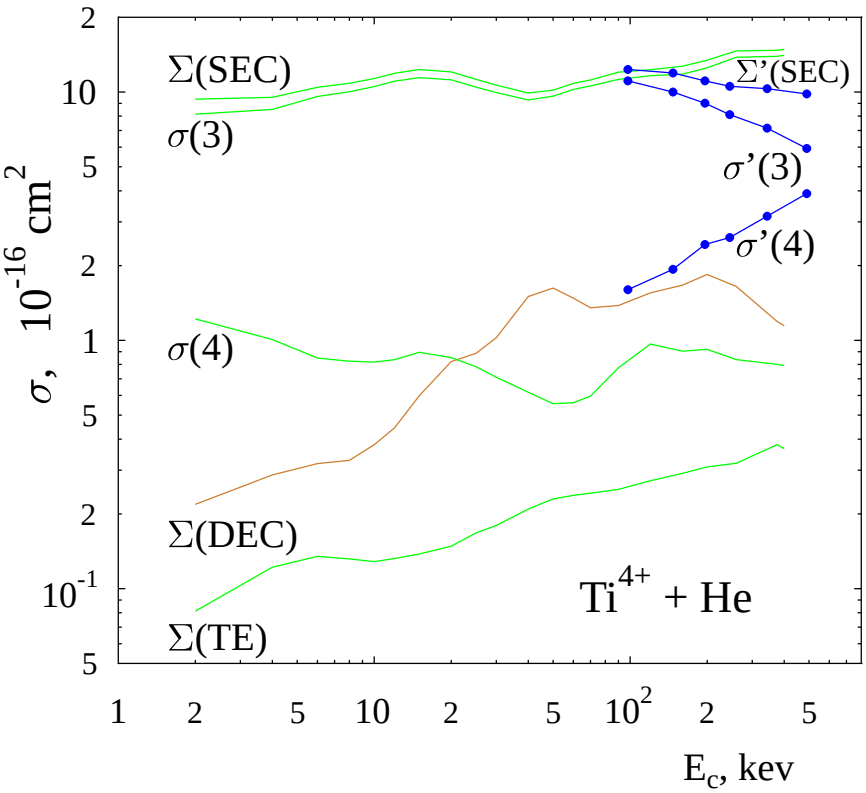

Figure 4: **The calculated cross sections as a function of the impurity ion energy E_c for the Ti^{4+} + He collisions:** $\Sigma(\mathrm{SEC})$ **– the total cross section of single-electron transfer** $(\sigma(3)+\sigma(4)+\sigma(\mathrm{TE}))$**;** $\sigma(3)$, $\sigma(4)$ **– the single-electron transfer cross section into n-shells with n=3 and n=4 of** Ti^{3+} **ions,** $\Sigma(\mathrm{TE})$ **– the transfer excitation cross section;** $\Sigma(\mathrm{DEC})$ **– double-electron capture cross section.** Σ'**(SEC),** $\sigma'(3)$ **and** $\sigma'(4)$ **– the results by Fritsch [13] (blue curves).**

b) Cr^{6+}–He, Fe^{8+}–He collisions

The calculated cross sections for Cr^{6+} + He($1s^2$) and for Fe^{6+} + He($1s^2$) in the energy range from 2 to 400 keV are shown in Fig. 5 and Fig. 6., respectively. The maximum value of the total single and double electron transfer cross sections obtained is equal 4.72×10^{-15} cm^2 (at $E_c \simeq 400$ keV) and 1.45×10^{-16} cm^2 (at $E_c \simeq 300$ keV) for Cr^{6+}– He collision. For Fe^{8+}– He collision the maximum value of the total single-electron transfer cross section obtained is equal 1.3×10^{-14} cm^2 at $E_c \simeq 400$ keV; the value of double electron transfer cross section is less than 1.3×10^{-17} cm^2.

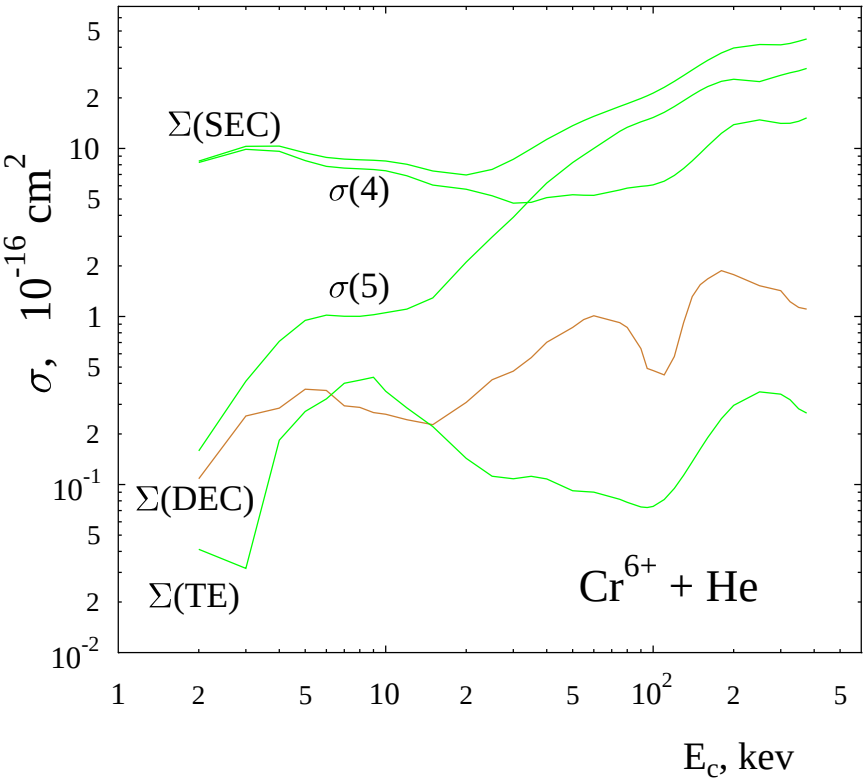

Figure 5: **The calculated cross sections as a function of the impurity ion energy E_c for Cr^{6+} + He collision: Σ(SEC) – the total cross section of single-electron transfer ($\sigma(4) + \sigma(5)$+TE); $\sigma(4)$ and $\sigma(5)$ – the single-electron transfer cross sections into n-shells with n=4 and n=5 of Cr^{5+} ions, Σ(TE) – the transfer excitation cross section; Σ(DEC) – the double-electron capture cross section.**

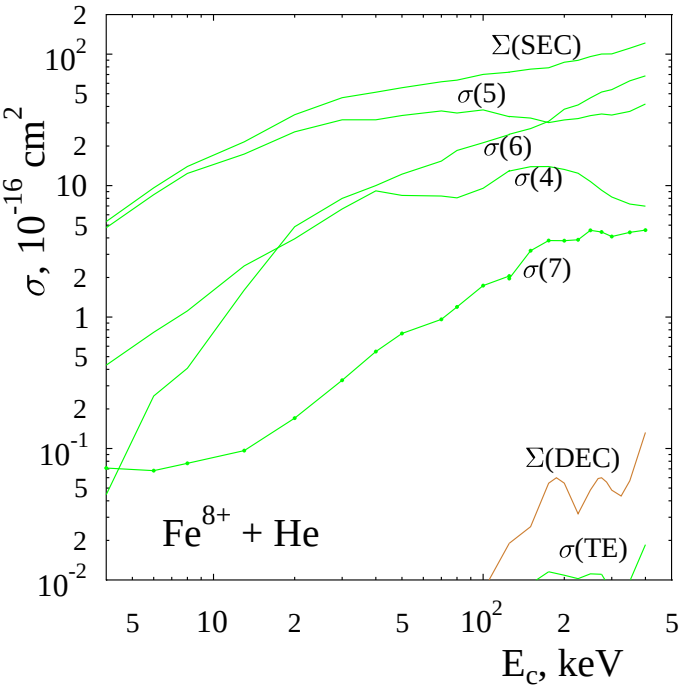

Figure 6: **The calculated cross sections as a function of the impurity ion energy E_c for Fe^{8+} + He collision: Σ(SEC) – the total cross section of single-electron transfer ($\sum_n \sigma(n)$+TE); $\sigma(n)$ – the single-electron transfer cross sections into n-shells with n=4–7 of Fe^{7+} ions, σ(TE)– the transfer excitation cross section; Σ(DEC) – the double-electron capture cross section.**

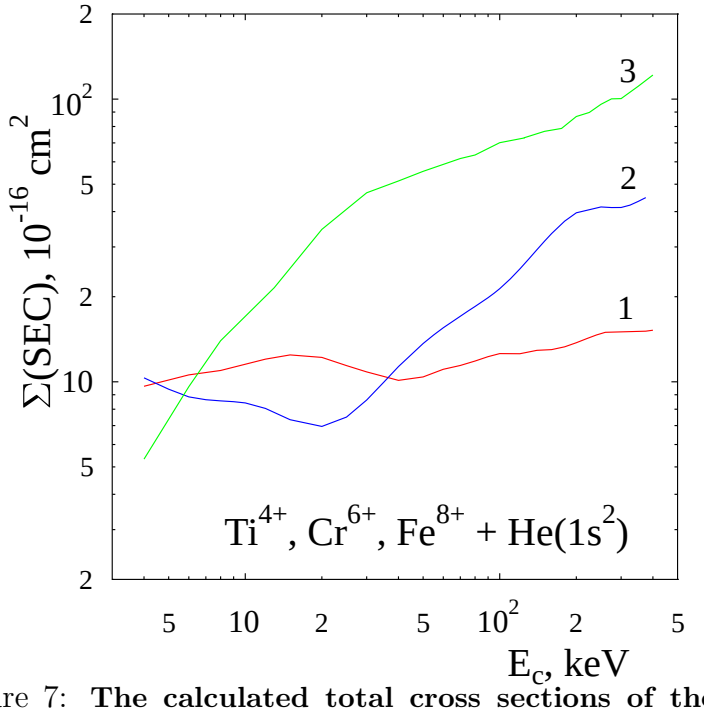

Figure 7: **The calculated total cross sections of the single-electron transfer as a function of the impurity ion energy E_c for collisions: 1 – Ti^{4+}+ He($1s^2$) 2 – Cr^{6+}+ He($1s^2$), 3 – Fe^{8+}+ He($1s^2$).**

4. Theoretical study of the single-electron charge transfer in collisions of Ti^{4+}, Cr^{6+}, and Fe^{8+} with helium atoms in the first excited state

The electron transfer and excitation in collisions between impurities and helium atoms in excited states of atomic beams used for edge and central plasma diagnostics could be important in the level population. According to R. Janev [14], atomic and ion species in metastable excited states have significant effects on the kinetics of partially ionized edge and divertor plasmas. The most important of the collision processes involving metastables and plasma impurity ions are those leading to the excitation of metastables or the electron capture.

Recently within IAEA projects a serious effort was made by theorists to determine the relevant cross sections involving light impurities.

The state selective and total cross sections for electron capture, excitation and ionization processes in slow collisions of H(2s) and He^+(2s) with light bare ions (Z=1–5) were calculated by R. Janev et al [14] by using the hidden crossing method.

Electron transfer and excitation cross sections have been determined by W. Fritsch and H. Tawara [15] for Be^{4+}– He collision with an initially excited He(1s2s) 2 ^{1}S target by using the close-coupling equation method with a one-electron AO expansion.

The classical trajectory Monte Carlo (CTMC) calculations of state selective SEC and EXC cross sections for collisions between excited helium and bare light ions (Z=3–6,8) were performed in the work [16].

We carried out [4, 5] the close coupling calculation of the single electron capture and excitation cross sections for slow collisions:

$$A^{q+}(3p^6) + He(1s2s) \rightarrow \begin{cases} A^{(q-1)+}(3p^6 n'l') + He^+(1s) & (SEC) \\ A^{q+}(3p^6) + He(1sn'l') \ (n' = 2,3) & (EXC) \end{cases}$$

(A=Ti, Cr, Fe; q=Z_A-18, Z_A=24, 26, 28 - the nuclear charges of the impurity ions).

The cross sections of the processes were calculated in terms of the close-coupling method in the basis of seventeen one-electron states for Ti^{4+} + He(1s2s) collision and ten states for Cr^{6+}, Fe^{8+} + He(1s2s) collisions.

The calculated one-electron screened state correlation diagrams for (Ti^{4+}+He^+(1s))e, (Cr^{6+}+He^+(1s))e, and (Fe^{8+}+He^+(1s))e quasimolecules are shown in Fig. 8 – 10.

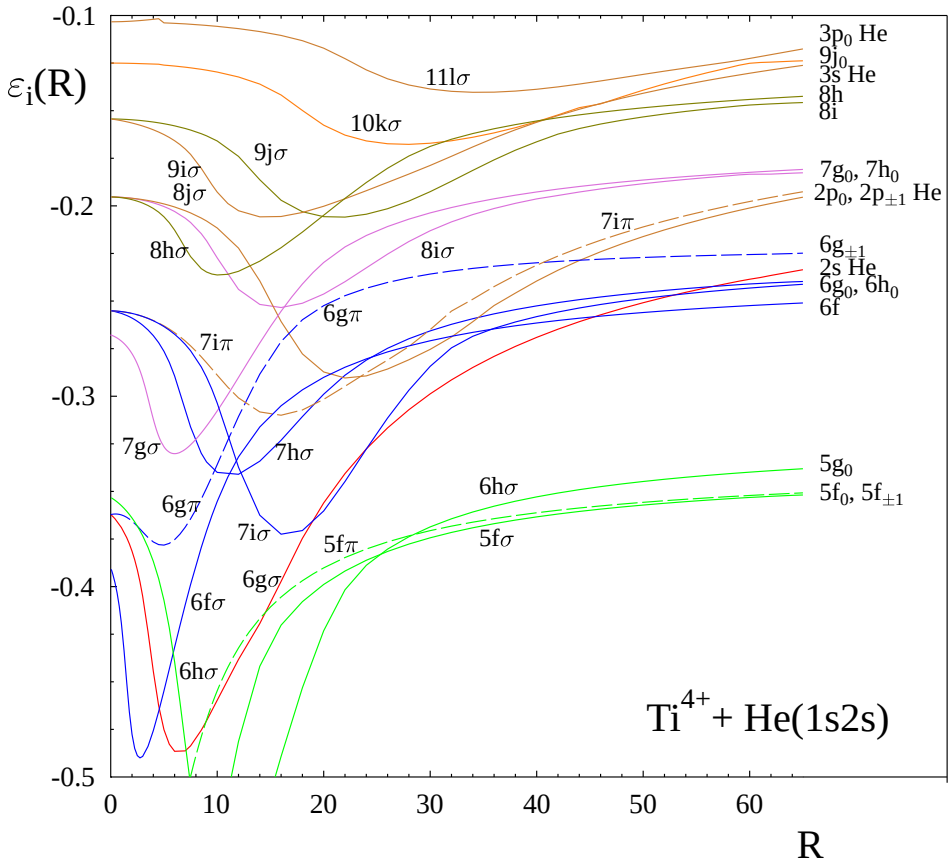

Figure 8: **The energies ε_j(R) of SDMO $\psi_j(r;\mathrm{R})$ of (Ti^{4+}+ He^{+}(1s))e quasimolecule and their atomic limits at R $\to \infty$.**

a) the entrance channel (red curve) – ψ_1=6gσ;

b) the channels of the single-electron transfer into nl-states of Ti^{3+} ions:

n=5 (green curves) – 5f$_0$-, 5f$_{\pm1}$-, and 5g$_0$-states (ψ_2=5fσ, ψ_3=5fπ, ψ_4=6hσ),

n=6 (blue curves) – 6f$_0$-, 6g$_0$-, 6g$_{\pm1}$-, 6h$_0$-states (ψ_5=6fσ, ψ_6=7hσ, ψ_7=6gπ, ψ_8=7iσ),

n=7 (orchid curves) – 7g$_0$-, 7h$_0$-states (ψ_9=7gσ, ψ_{10}=8iσ),

n=8 (olive curves) – 8h$_0$-, 8i$_0$-states (ψ_{11}=8hσ, ψ_{12}=9jσ),

n=9 (orange curve) – 9j$_0$-state (ψ_{13}=10kσ);

c) the channels of the electron 2s$\to$ nl excitation of He(1s2s) atoms (gold curves):

nl=2p$_0$, 2$p_{\pm1}$ (ψ_{14}=8jσ, ψ_{15}=7iπ),

3s, 3p$_0$ (ψ_{16}=9iσ, ψ_{17}=11lσ).

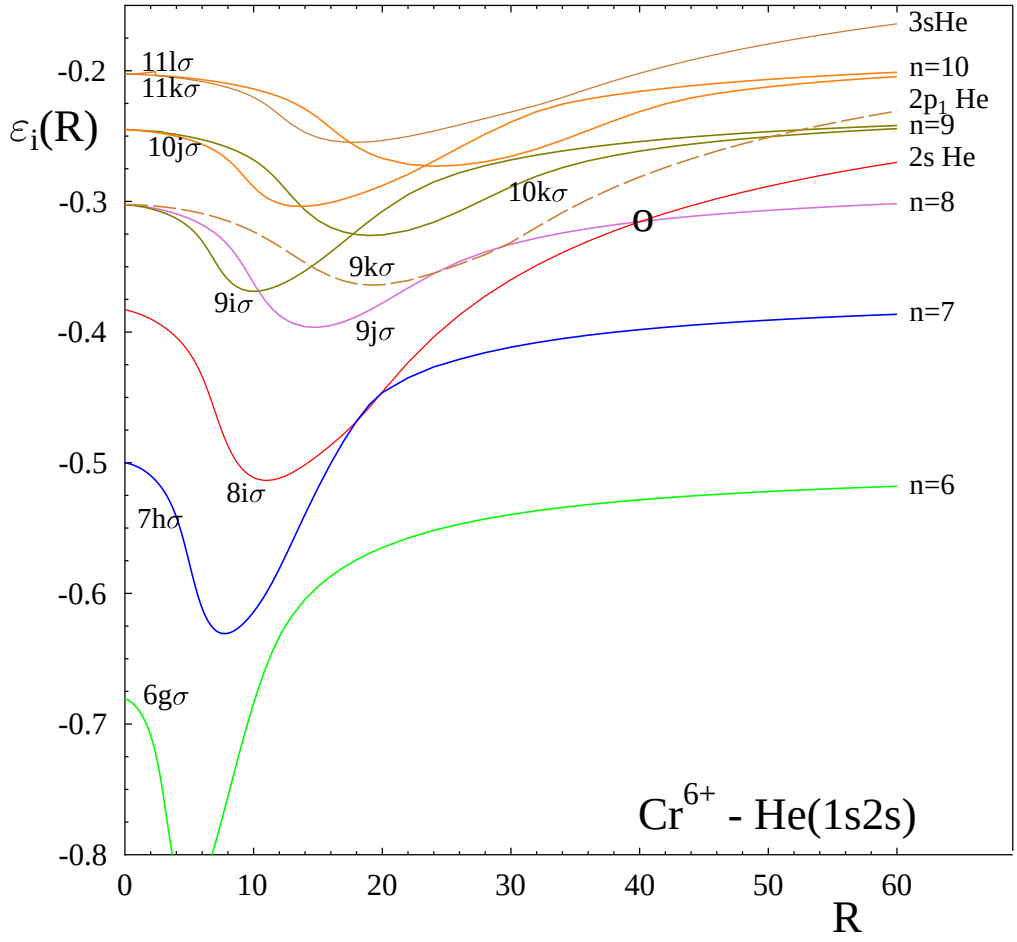

Figure 9: **The energies ε_j(R) of SDMO $\psi_j(r;\mathrm{R})$ of (Cr^{6+}+ He^{+}(1s))e quasimolecule and their atomic limits at R $\to \infty$.**

a) the entrance channel (red curve) – ψ_1=8iσ;

b) the channels of the single-electron transfer into nl-states of Cr^{5+} ions:

n=6 (green curve) – 6g$_0$-state (ψ_2=6gσ),

n=7 (blue curve) – 7h$_0$-state (ψ_3=7hσ),

n=8 (orchid curve) – 8i$_0$-states (ψ_4=9jσ),

n=9 (olive curves) – 9i$_0$-, 9j$_0$-states – (ψ_5=9iσ, ψ_6=10kσ),

n=10 (orange curve) –10j$_0$-, 10k$_0$-states (ψ_7=10jσ, ψ_8=11lσ);

c) the channels of electron 2s$\to$ nl excitation of He(1s2s) atoms (gold curves):

nl=3s (ψ_9=11kσ),

2$p_{\pm 1}$ (ψ_{10}=9kπ).

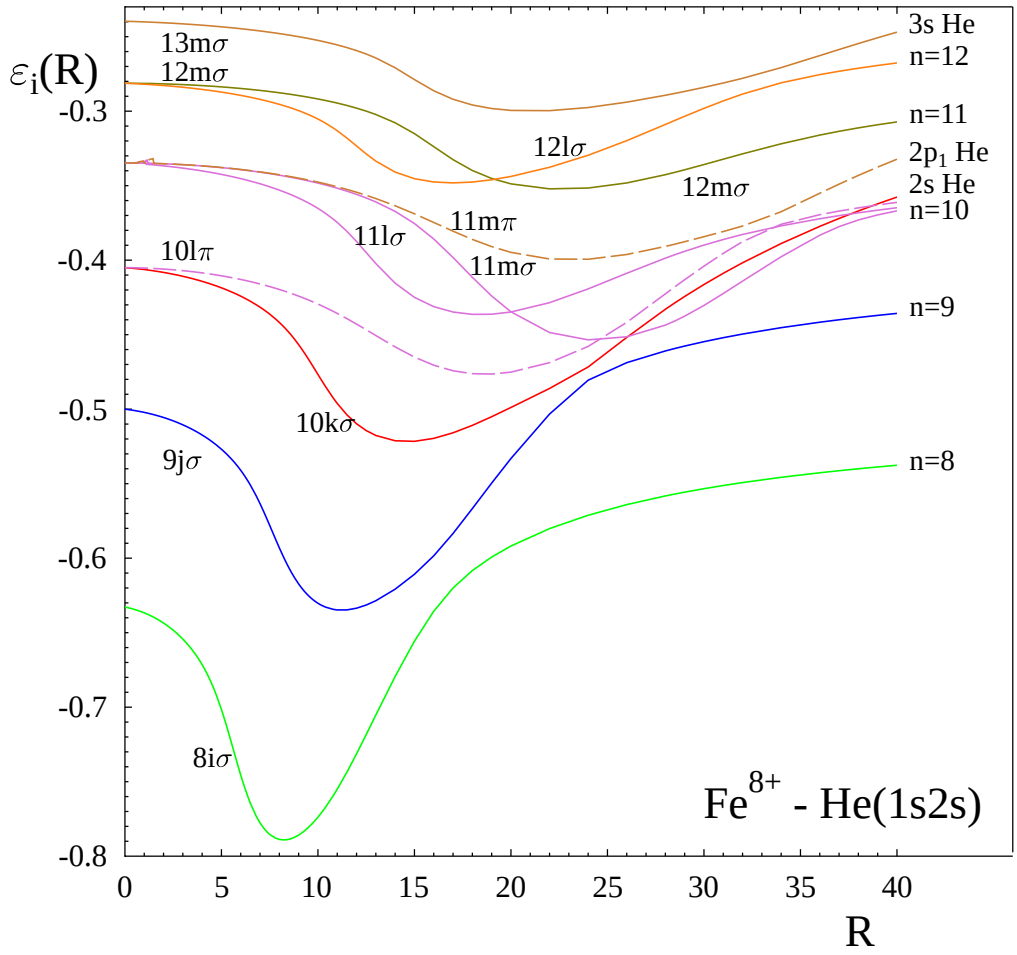

Figure 10: **The energies ε_j(R) of SDMO $\psi_j(r;\mathrm{R})$ of (Fe^{8+}+ He^{+}(1s))e quasimolecule and their atomic limits at R $\to \infty$.**
a) the entrance channel (red curve) – ψ_1=10kσ;
b) the channels of single-electron transfer into nl-states of Fe^{7+} ions:
n=8 (geen curve) – 8i$_0$-state (ψ_2=8iσ),
n=9 (blue curve) – 9j$_0$-state (ψ_3=9jσ),
n=10 (orchid curves) – 10k$_0$-, 10l$_0$-, 10l$_{\pm1}$ -states (ψ_4=11lσ, ψ_7=11mσ, ψ_8=10lπ),
n=11 (olive curve) – 11l$_0$- state (ψ_5=12mσ),
n=12 (orange curve) – 12l$_0$-state (ψ_{10}=12lσ);
c) the channels of electron 2s→ nl excitation of He(1s2s) atoms (gold curves):
nl= 3s (ψ_6=13mσ),
2$p_{\pm1}$ (ψ_9=11mπ).

Results obtained

Results of our theoretical study of the single electron charge transfer in collisions of Ti^{4+}, Cr^{6+} and Fe^{8+} with helium atoms in the first excited state were published in [4, 5].

The cross sections of electron transfer to nl-states on Ti^{3+} ion (n=5-8) and of the electron He(2s→3l) excitation in collisions of the excited helium atoms He(1s2s) and the Ti^{4+} ions were obtained in the range of the ion energy E$_c$ 5 –300 keV. The data are shown in graphical form (Fig. 11-13). The

maximum values of the total electron transfer and excitation cross sections were obtained equal 2.05 10^{-14} cm^2 and 7.70 10^{-16} cm^2 (at E_c=300 keV) for Ti^{4+} + He collision, 2.32 10^{-14} cm^2 and 2.00 10^{-15} cm^2 (at E_c=400 keV) for Cr^{6+}+ He collision, and 3.40 10^{-14} cm^2 and 9.54 10^{-15} cm^2 (at E_c=400 keV) for Fe^{8+}+ He collision, appropriately.

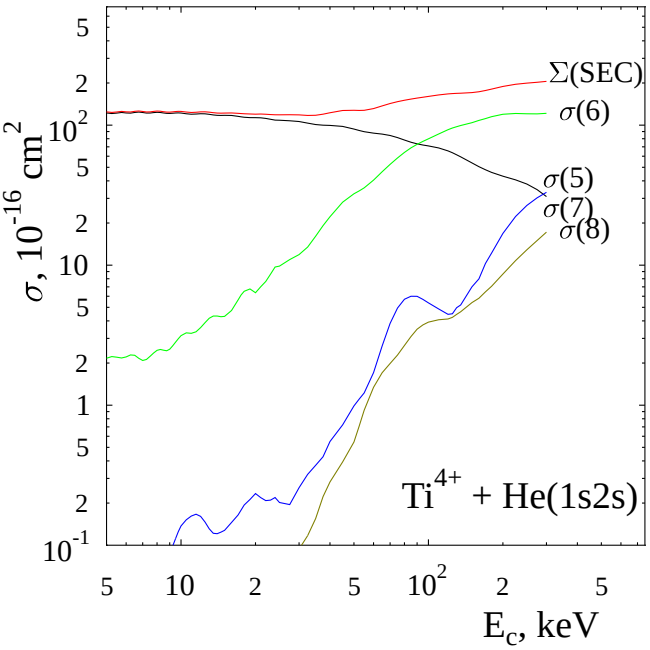

Figure 11: **The calculated cross sections as a function of the impurity ion energy E_c for Ti^{4+}+He(1s2s) collision: Σ(SEC) – the total electron transfer cross section, $\sigma(n)$ – electron transfer cross sections into n-shells with n=6–8 of Ti^{3+} ions.**

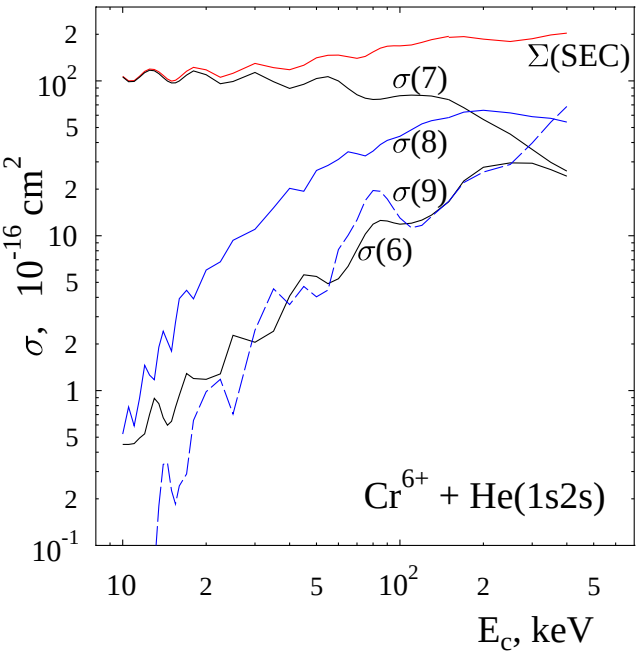

Figure 12: **The calculated cross sections as a function of the impurity ion energy $\mathbf{E}_c$ for $\mathbf{Cr^{6+}}$+He(1s2s) collisions: Σ(SEC) – the total cross section of the single-electron transfer; $\sigma(n)$ – the single-electron cross sections into n-shells with n=6-9 of $\mathbf{Cr^{5+}}$ ions.**

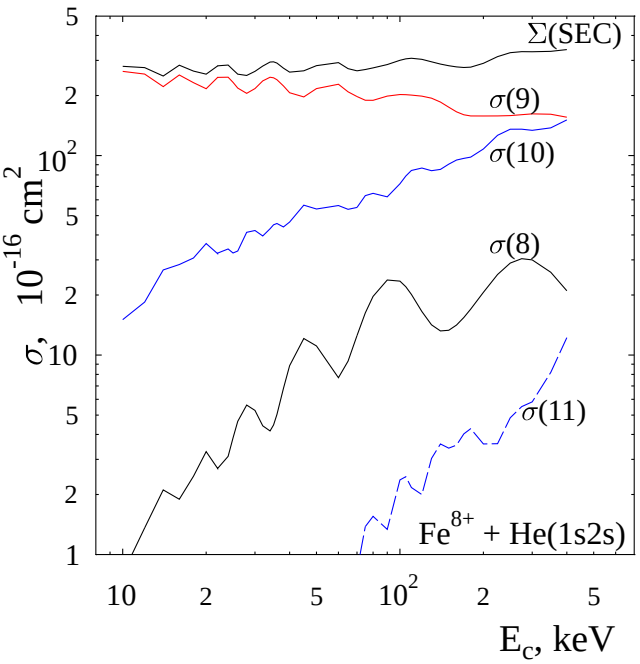

Figure 13: **The calculated cross sections as a function of the impurity ion energy E_c for Fe^{8+}+He(1s2s) collision: Σ(SEC) – the total cross section of the single-electron transfer; $\sigma(n)$ – the single-electron cross sections into n-shells with n=8-11.**

Calculated n-distribution of the electron transfer cross section for Ti^{4+}, Cr^{6+}, Fe^{8+}– He(1s2s) collisions are shown in Fig. 14–16. In Fig. 14 we compare the calculated n-distribution in Ti^{4+} – He(1s2s) collision at 240 keV (5 keV/u) with results by Fritsch and Tawara [15] for Be^{4+} – He(1s2s) collisions. The agreement is only qualitative because we have Ti^{4+} ion with the Ar-like core but no bare ion.

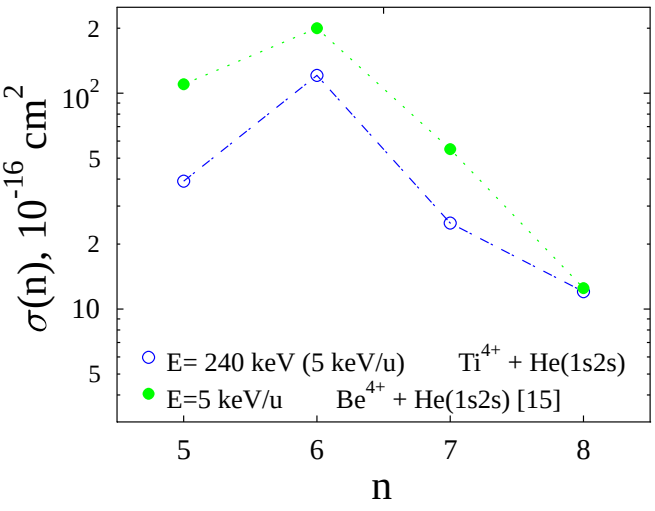

Figure 14: **n-distribution of electron transfer cross sections in Ti^{4+}+ He(1s2s) collision from our calculation (blue curve) and in Be^{4+}+ He(1s2s) from [15] (green curve) at 5 keV/u.**

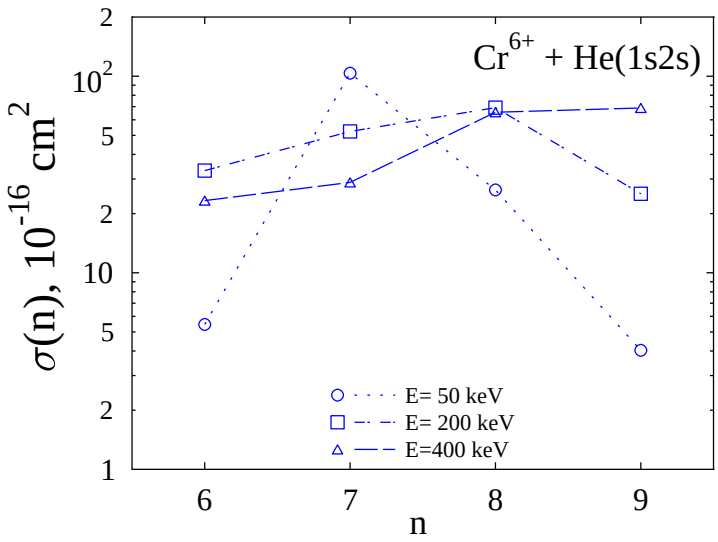

Figure 15: **Calculated n-distribution of electron transfer cross section in Cr^{6+}+ He(1s2s) collision.**

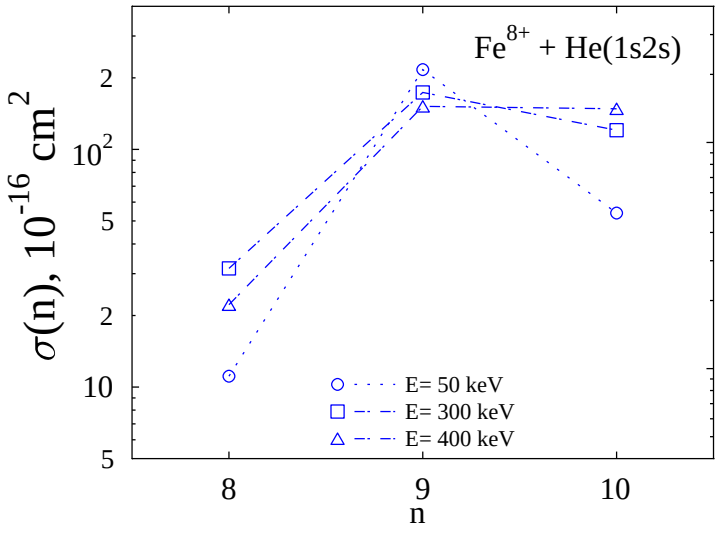

Figure 16: **Calculated n-distribution of electron transfer cross section in Fe^{8+}+ He(1s2s) collision.**

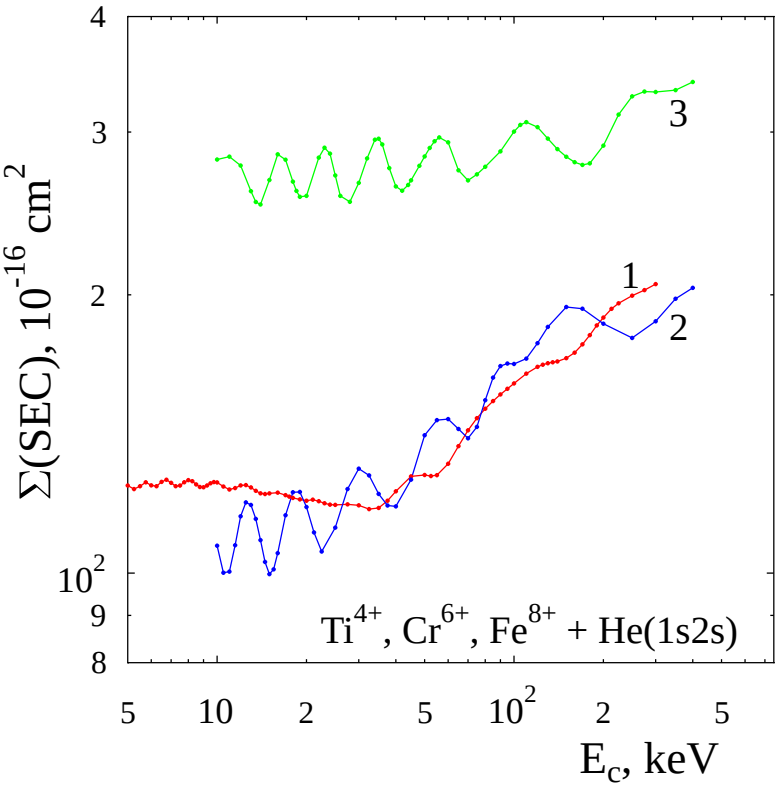

Figure 17: **Calculated total cross sections of the single-electron transfer as a function of the impurity ion energy E_c for collisions: 1 – Ti^{4+}+ He(1s2s) 2 – Cr^{6+}+ He(1s2s), 3 – Fe^{8+}+ He(1s2s).**

The charge transfer cross sections in the collisions of impurity ions with metastable helium atoms are of the order of magnitude larger than the corresponding cross sections for the ground-state helium. A small admixture of metastable helium in a neutral beam can hence considerable change the spectra of charge-exchange spectroscopy.

5. Study of alpha particle neutralization through quasi-resonant double electron capture in slow collisions with C^{2+} and Ti^{2+} ions.

The energy loss due to photon emission from metallic impurity ions excited through charge-exchange collisions with the hydrogen or helium atoms is a serious problem in fusion reactors. Destruction of ground and especially excited states of abundant neutral atomic and molecular hydrogen and the He atoms by SEC and DEC in their collisions with metallic impurity ions are the most important processes in the edge plasmas.

Previously the key role of the alpha-particle neutralization reactions in cooling the edge plasmas was discussed by Tawara [17]. The reactions are due to DEC into metastable $He^{o}(1s3l)$ state at collisions of alpha-particles with H_2 in low eV-energies. On the other hand, DEC cross sections in this collisions into the $He^{o}(1s^2)$ ground state are known to be small contrary to our case.

In slow ion-atom collisions, SEC reactions are generally dominant inelastic channels with only one exception – the collision system C^{4+}– He. DEC dominates over SEC at collision energies below 20 keV, according to Grandall [18] for collisions:

$$C^{4+}(1s^2) + He(1s^2) \rightarrow \qquad C^{2+}(1s^2 2s^2) + He^{2+} \qquad (3)$$

It would appear reasonable that DEC would dominate over SEC for the inverse ion-ion reaction. Calculations for this reaction were carried out using the method of close-coupling equations with the basis set of nine quasimolecular four-electron states. Energies of many-electron diabatic and adiabatic states and matrix elements (dynamic and potential) were calculated by using our program package for treatment of inelastic processes at ion-atom collision in a framework of the quasimolecular approach.

Results of our calculation of the DEC cross section for direct reaction (3), using six four-electron quasimolecular states in the close-coupling equation set, are shown in Fig. 18. In the high velocity limit, there is agreement between all theoretical results and experiment. It is clearly seen that at low energies, our results are in better agreement with experimental data.

The DEC cross section values for Ti^{4+} + He collisions (Fig. 4) are less than those for C^{4+} + He collisions (Fig.18) by a factor of 2.5. Consequently, the cross sections of alpha particle neutralization through quasi-resonant double-electron capture at their slow collisions with C^{2+} and Ti^{2+} are differ by the same factor (see Fig. 19).

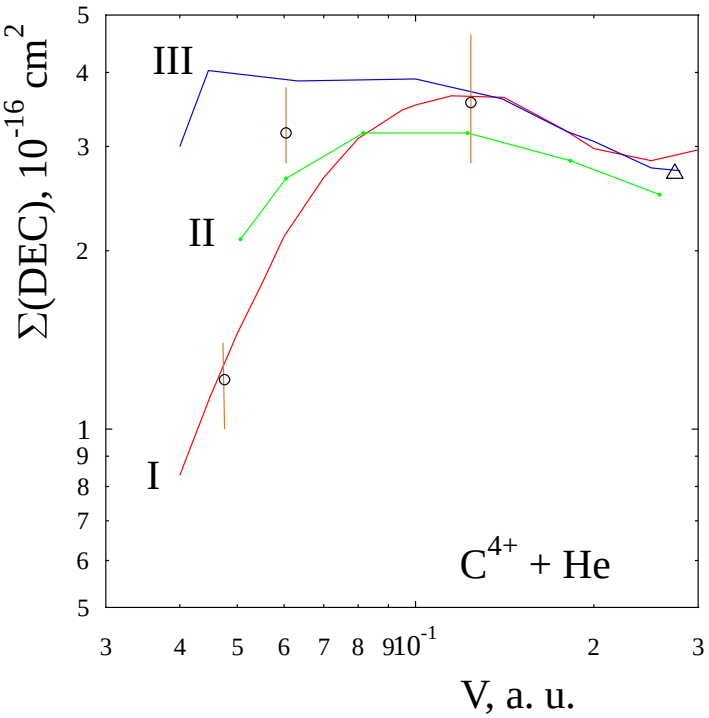

Figure 18: **Total double-electron capture cross sections for $C^{4+} + He \rightarrow C^{2+} + He^{2+}$ collision as a function of the relative velocity V. Theoretical results: I – present results; II – results of Kimura and Olson [19], III – results of Errea et al [20]. Experimental data: (o) data of Phaneuf and Grandall [21]; (Δ) data by Grandall [18].**

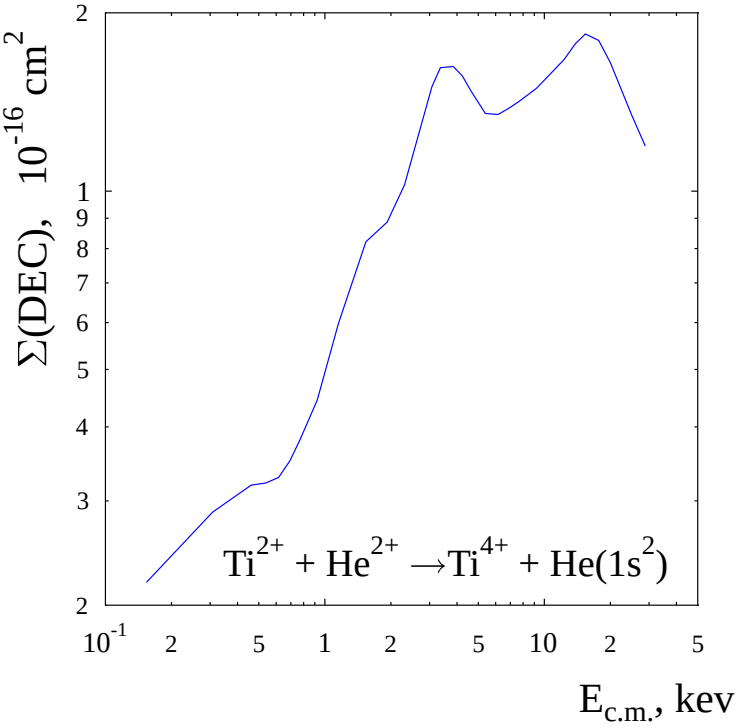

Figure 19: **Total double-electron capture cross sections for $Ti^{2+} + He^{2+}$ collision as a function of the center of mass collision energy $E_{c.m.}$.**

6. Electron capture and excitation processes in collisions of alpha particles with Be-like oxygen ions.

The following reactions for collisions between alpha particles and the O^{4+} ions were considered for the first time [6]

$$He^{2+} + O^{4+}(1s^2 2s^2) \rightarrow \begin{cases} He^{+}(n'l') + O^{5+}(1s^2 2s) & n' = 1,2 \quad (1) \\ He^{+}(n'l') + O^{5+}(1s^2 2p) & n' = 1,2 \quad (2) \\ He^{2+} + O^{4+}(1s^2 2lnl) & n = 2-4. \quad (3) \end{cases}$$

The cross sections for reaction of electron transfer (1), transfer excitation (2) and target excitation (3) were calculated by solving close-coupling equations using the basis set of thirteen quasimolecular four-electron states.

Table IV. Entrance, electron transfer, transfer excitation, target single-electron excitation (SE EXC) and double-electron excitation (DE EXC) channels. Energies of resonance defects ΔE_p are obtained from atomic calculations.

channel	Φ_p	**atomic limit at R** $\rightarrow \infty$	ΔE_p **(a.u.)**
DE EXC	Φ_9	$\mathbf{He^{2+} + O^{4+}}(1s^2 2p4f)$	ΔE_9**=3.84**
	Φ_7	$\mathbf{He^{2+} + O^{4+}}(1s^2 2p3d)$	ΔE_7**=3.19**
	Φ_3	$\mathbf{He^{2+} + O^{4+}}(1s^2 2p^2)$	ΔE_3**=0.96**
SE EXC	Φ_8	$\mathbf{He^{2+} + O^{4+}}(1s^2 2s4f)$	ΔE_8**=3.41**
	Φ_6	$\mathbf{He^{2+} + O^{4+}}(1s^2 2s3d)$	ΔE_6**=2.75**
	Φ_2	$\mathbf{He^{2+} + O^{4+}}(1s^2 2s2p)$	ΔE_2**=0.48**
transfer excitation	Φ_{12}, Φ_{13}	$\mathbf{He^{+}(2l) + O^{5+}}(1s^2 2p)$	$\Delta E_{14,15}$**=3.97**
	Φ_5	$\mathbf{He^{+}(1s) + O^{5+}}(1s^2 2p)$	ΔE_5**=2.47**
electron transfer	Φ_{10}, Φ_{11}	$\mathbf{He^{+}(2l) + O^{5+}}(1s^2 2s)$	$\Delta E_{10,11}$**=3.59**
	Φ_4	$\mathbf{He^{+}(1s) + O^{5+}}(1s^2 2s)$	ΔE_4**=2.05**
entrance	Φ_1	$\mathbf{He^{2+} + O^{4+}}(1s^2 2s^2)$	

Results obtained

The partial cross sections for all exit channels from Table IV were calculated by solving the close coupling equations in the energy range of incident the He^{2+} ions from 0.2 to 2 MeV.

The main electron transfer process is transfer into 1s state of He^{+}(1s) ion (exit channels Φ_4, Φ_{10}, Φ_{11} from Table IV). The simultaneous transfer and excitation (TE) of two electrons (exit channels Φ_5, Φ_{12}, Φ_{13}) in He^{2+}–$O^{4+}(1s^2 2s^2)$ collision is an example of the correlation process. It was found that this TE process is of more importance than the electron transfer into excited state of the He^{+}(2p) ion. The maximum value of the total electron transfer and TE processes was obtained equal $\sim$ 2.2$\times 10^{-16}$ cm^2 at alpha-particle energy $\sim$ 0.7 MeV (see Fig. 20).

The total excitation cross section as a function of the collisional energy has two humped structure (see Fig. 21). There is a maximum due to single-electron excitations ($\sim$ 7.7$\times 10^{-16}$ cm^2) at energy $\sim$ 80 keV and a feebly marked maximum ($\sim$ 6.5$\times 10^{-16}$ cm^2) at energy $\sim$ 0.7 MeV due to double-electron excitations.

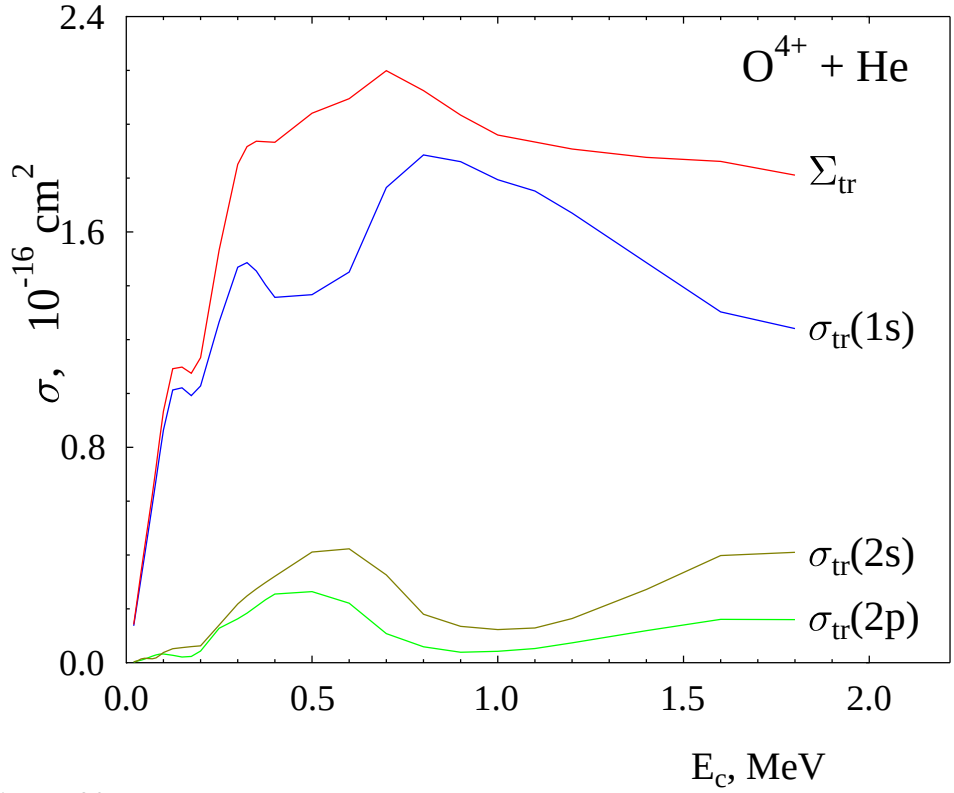

Figure 20: **The total electron transfer and transfer excitation cross section Σ_{tr}. The partial cross sections $\sigma_{tr}(nl)$ of single-electron transfer into nl-states of He^{+} ion with simultaneous electron 2s→2p excitation of target in the He^{2+}– O^{4+} collision.**
$\sigma_{tr}(1s)$=σ_4 + σ_5, $\sigma_{tr}(2s)$=σ_{10} + σ_{12}, $\sigma_{tr}(2p)$=σ_{11} + σ_{13} (see Table IV).

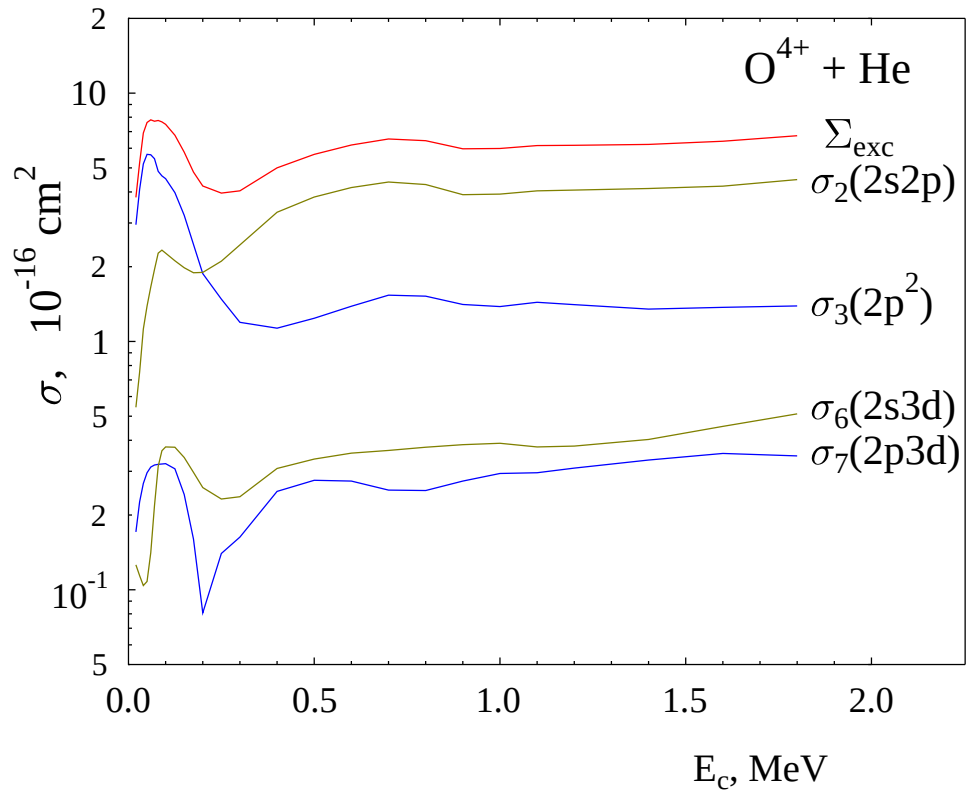

Figure 21: **The cross sections of target excitation as a function of the collisional energy in the He^{2+}– O^{4+} collision: Σ_{exc} – the total cross section of excitation into 2lnl states with n=2,3 of O^{4+} ions; σ_2(2s2p), σ_6(2s3d) – the partial cross sections of the single-electron excitation into 2s2p and 2s3d states of O^{4+} ions (SE EXC, olive curves); σ_3($2p^2$), σ_7(2p3d) – the partial cross sections of double-electron excitation into $2p^2$ and 2s3d states of O^{4+} ions (DE EXC, blue curves).**

7. Theoretical study of charge transfer and excitation in slow collisions between Bi^{4+} ions in the ground and metastable states

The processes of single-electron charge transfer (reactions 1a and 1b) and excitation (process 1c) occuring in collisions between the Bi^{4+} ions in the ground state for the singlet and triplet channels and in collisions between ions in the ground and metastable states for both the singlet and triplet entrance channels (reactions 2) were considered [7, 8]:

$$
{}^2\mathrm{S}\ \mathrm{Bi}^{4+}(6\mathrm{s}) + {}^2\mathrm{S}\ \mathrm{Bi}^{4+}(6\mathrm{s}) \rightarrow \begin{cases} {}^1\mathrm{S}\ \mathrm{Bi}^{3+}(6\mathrm{s}^2) + {}^1\mathrm{S}\ \mathrm{Bi}^{5+}(5\mathrm{d}^{10}), & \Delta\mathrm{E} = 11.16\ \mathrm{eV} \quad (1a) \\ {}^3\mathrm{P}\ \mathrm{Bi}^{3+}(6\mathrm{s}6\mathrm{p}) + {}^1\mathrm{S}\ \mathrm{Bi}^{5+}(5\mathrm{d}^{10}), & \Delta\mathrm{E} = 21.15\ \mathrm{eV} \quad (1b) \\ {}^2\mathrm{P}\ \mathrm{Bi}^{4+}(6\mathrm{p}) + {}^2\mathrm{S}\ \mathrm{Bi}^{4+}(6\mathrm{s}), & \Delta\mathrm{E} = 10.71\ \mathrm{eV}. \quad (1c) \end{cases}
$$

$$
{}^2\mathrm{S}\ \mathrm{Bi}^{4+}(6\mathrm{s}) + {}^2\mathrm{P}\ \mathrm{Bi}^{4+}(6\mathrm{p}) \rightarrow \begin{cases} {}^{1,3}\mathrm{P}\ \mathrm{Bi}^{3+}(6\mathrm{s}6\mathrm{p}) + {}^1\mathrm{S}\ \mathrm{Bi}^{5+}(5\mathrm{d}^{10}), & \Delta\mathrm{E} = 10.44\ \ \mathrm{eV} \quad (2a) \\ {}^1\mathrm{S}\ \mathrm{Bi}^{3+}(6\mathrm{s}^2) + {}^1\mathrm{S}\ \mathrm{Bi}^{5+}(5\mathrm{d}^{10}), & \Delta\mathrm{E} = 0.46\ \ \mathrm{eV} \quad (2b) \\ {}^2\mathrm{P}\ \mathrm{Bi}^{4+}(6\mathrm{p}) + {}^2\mathrm{S}\ \mathrm{Bi}^{4+}(6\mathrm{s}), & \Delta\mathrm{E} = 0 \quad (2c) \end{cases}
$$

Results obtained

The cross sections of the processes are calculated by the close-coupling equation method in the basis of two electron quasimolecular states (see Fig. 22 – $\mathrm{E_{c.m.}}$ is the center of mass collision energy). It is found that SEC into the singlet states of the ^{1}S Bi$^{3+}(6s^2)$ ions makes a major contribution to the cross section for the Bi^{4+}(6s)+Bi^{4+}(6s) collisions, whereas SEC into the singlet states ^{1}P Bi^{3+}(6s6p) is the basic contribution to the cross section in the Bi^{4+}(6s)+Bi^{4+}(6p) collisions.

The fraction of metastable ions in the beams is estimated by comparing theoretical and experimental results for the charge transfer total cross sections. The dashed line in Fig. 22 refers to the charge transfer total cross section in the case when fractions of reactions I and II are 0.6 and 0.4 respectively. Such a proportion implies that the fraction of metastable ions amounts to 20% in either of crossed beams.

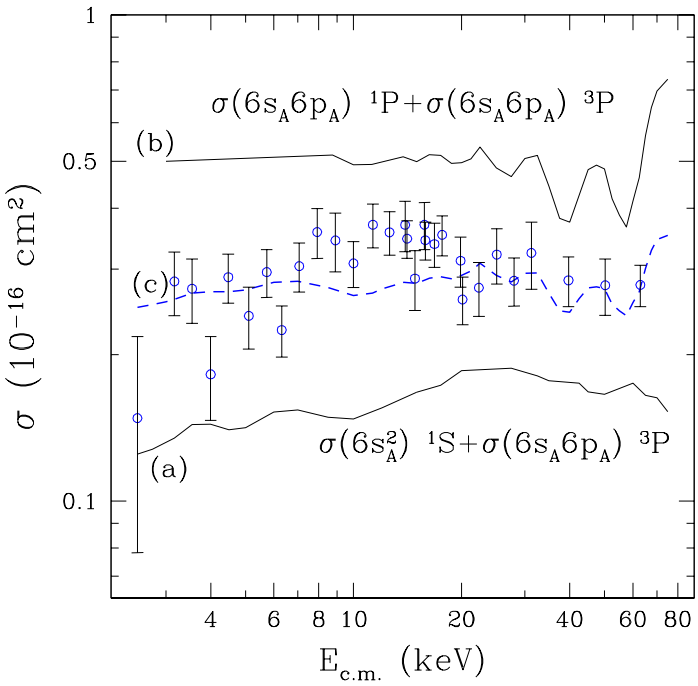

Figure 22: **Statistically weighted total charge transfer cross sections for the singlet and triplet exit channels in (a) Bi^{4+}(6s)-Bi^{4+}(6s) and (b) Bi^{4+}(6s)-Bi^{4+}(6p) collisions. (c) The weighted average charge transfer cross section for fractions of reactions (a) and (b) of 0.6 and 0.4 – dashed line. (○) Total transfer cross section obtained in crossed-beam experiments [22].**

Citation of periodical reporting work done under this CRP

[1] V. K. Nikulin, N. A. Guschina. Electron transfer and excitation in collisions between heavy element impurity ions and helium atoms. I. Ti^{4+} – He collisions. Report of Ioffe Physico-Technical Institute N 1789 (2006) 23 p.

[2] V. K. Nikulin, N. A. Guschina. Electron transfer and excitation in collisions between Ti^{4+}, Cr^{6+} ions and helium atoms. Report of Ioffe Physico-Technical Institute N 1791 (2006) 45 p.

[3] V. K. Nikulin, N. A. Guschina. Electron transfer and excitation in collisions between Fe^{8+} ions and helium atoms. Report of Ioffe Physico-Technical Institute N 1792 (2007) 27 p.

[4] V. K. Nikulin, N. A. Guschina. State-selective and total electron transfer and excitation cross sections in slow collisions of excited He(1s2s) atoms and Ti^{4+}, Cr^{6+}, Fe^{8+} ions. I. Ti^{4+}– He(1s2s) collision. Report of Ioffe Physico-Technical Institute N 1793 (2007) 35 p.

[5] V. K. Nikulin, N. A. Guschina. State-selective and total electron transfer and excitation cross sections in slow collisions of excited He(1s2s) atoms and Ti^{4+}, Cr^{6+}, Fe^{8+} ions. II. Cr^{6+}, Fe^{8+}– He(1s2s) collisions. Report of Ioffe Physico-Technical Institute N 1794 (2007) 34 p.

[6] V. K. Nikulin, N. A. Guschina. Cross sections for charge transfer and excitation in alpha-particle collisions with Be-like oxygen impurity ions in plasma. Technical Physics, 51, 1276 (2006)

[7] V. K. Nikulin, N. A. Guschina. Single-electron charge transfer and excitations at collisions between Bi^{4+} ions in the kiloelectronvolt energy range. Technical Physics, 52, 148 (2007).

[8] V. K. Nikulin, N. A. Guschina. Theoretical stydy of charge transfer and excitation in slow collisions between Bi^{4+} ions in the ground and metastable states. XXV ICPEAC, Book of Abstracts, Freiburg, 2007, Mo 082.

Other relevant literature references

[9] I. Hofmann, Nucl. Instrum. Methods A 464, 24 (2001).

[10] N. A. Guschina, V. K. Nikulin. The program package for inelastic process computation in slow ion-atom collisions. Report of Ioffe Physico-Technical Inst. N 1717 (1998) 66 p.

[11] R. D. Piacentini, A. Salin, Computer Phys. Comm. 12, 199 (1976).

[12] V. K. Nikulin, N. A. Guschina. Diabatic correlation diagrams for quasimolecular description of ion-atom collisions. J. Phys. B: Atom and Molec. Phys. 11, 3553 (1978).

[13] W. Fritsch. APID 6, 131 (1995).

[14] R.K. Janev, E.A. Solov'ev, J.A. Stephens. State-Selective and Total Electron Capture, Excitation and Ionization Cross Sections in Slow Collisions of H(2s) and He^+(2s) with H^+, He^{2+}, Li^{3+}, Be^{4+}, and B^{5+}. IAEA, INDC(NDS)-393, 1999, Vienna.

[15] W. Fritsch and H. Tawara. Present Status on Atomic and Molecular DATA Relevant to Fusion Plasma and Modeling. NIFS–DATA–39, 1997, p.89.

[16] L. Salasnich, F. Sattin, Phys. Rev. A 51 (1995) 4281.

[17] H.Tawara. Roles of Atomic and Molecular Processes in Fusion Plasma Researches. NIFS–DATA–25, 1995.

[18] D. H. Crandall, Phys. Rev. A 16, 958 (1977).

[19] M. Kimura and R. E. Olson, J. Phys. B: Atom. Mol. Phys. 17, 713 (1984).

[20] L. F. Errea, B. Herrero, L. Mendes and A. Riera, J. Phys. B: Atom. Mol. Phys. 28, 693 (1995).

[21] R. A. Phaneuf and D. H. Crandall, 1981.

[22] A. Diehl, H. Brauning, R. Trassl, D. Hathiramani, A. Theiss, H. Kern, E. Salzborn, and I. Hofmann, J Phys. B 34, 4073 (2001).